

Exact finite-size scaling functions for the interfacial tensions of the Ising model on planar lattices

Ming-Chya Wu*

Institute of Physics, Academia Sinica, Nankang, Taipei 11529, Taiwan

(Received 15 November 2005; revised manuscript received 11 March 2006; published 27 April 2006)

Exact finite-size scaling functions of the interfacial tensions are obtained for the Ising model with isotropic coupling on a set of $M \times N$ planar lattices, including square (sq), plane triangular (pt), and honeycomb (hc) lattices. The analyses of transitive behaviors at criticality revise the knowledge of the interfacial tensions as a function of the aspect ratio defined by $R=M/N$ for R approaching to zero gradually. The amplitudes of the interfacial tensions for the sq, pt, and hc lattices are further shown to have relative proportions $1:\sqrt{3}/2:\sqrt{3}$ which are related to the aspect ratios for the three lattices to have similar domains.

 DOI: [10.1103/PhysRevE.73.046135](https://doi.org/10.1103/PhysRevE.73.046135)

PACS number(s): 05.50.+q, 75.10.-b, 64.60.Cn

The analysis of finite-size effects is an important issue in the experiments and in numerical studies of critical systems [1]. The scaling behaviors of such corrections to the properties of infinite systems play an increasingly important role in our theoretical understanding of the critical regime of statistical systems. Therefore, there have been many investigations on finite-size scaling, finite-size corrections, universal finite-size scaling functions (UFSSF's), and boundary effects for critical model systems in recent decades [1–8].

Recently, Wu *et al.* [8] used the exact partition functions of the Ising model on finite square (sq), plane triangular (pt), and honeycomb (hc) lattices with periodic-aperiodic boundary conditions [9] and the corresponding finite-size corrections [6], and extended the method of Ref. [10] to investigate the finite-size functions of the system. They obtained exact universal finite-size scaling functions for the specific heat, internal energy, and free energy on these lattices with exact nonuniversal metric factors [8]. The study resolves the difficulty that most of previous analyses of UFSSF's were based on numerical simulations which always have some numerical uncertainties in the obtained results. In this paper, based on the same analytical background, we extend the studies to the interfacial tension with isotropic coupling.

The interfacial tension is defined as the difference between the free energies of two finite-size systems with different boundary conditions [11–13]. For the case of the Ising model on $M \times N$ planar lattices, the interfacial tension is defined as the difference in free energy between systems with periodic and antiperiodic boundary conditions along the vertical direction as shown in Fig. 1 [12,13], which is also known as the Bloch wall free energy [11]. The interfacial tension in this paper is then defined as

$$\sigma(\epsilon, R, N) = M[f^{ap}(\epsilon, R, N) - f^{pp}(\epsilon, R, N)], \quad (1)$$

where $\epsilon=(T-T_c)/T_c$ is the reduced temperature, T is the absolute temperature, T_c is the critical temperature, $R=M/N$ is the aspect ratio, and the superscript a denotes antiperiodic boundary condition, and p for periodic boundary. According to Ref. [9], the free energy of the system defined as

$f^B = -(1/MN)\ln Z^B$, with partition function Z^B , can be written as

$$f^B = \frac{1}{MN} \left(1 - \frac{1+g}{2} MN \right) \ln 2 - \frac{1}{2} \ln[\sinh(2\eta)] - \frac{1}{MN} \ln \sum_{i=1}^4 \epsilon_i^B Z_i, \quad (2)$$

where the superscript B denotes the boundary conditions, $g=1$ for the sq and pt lattices, and $g=1/2$ for the hc lattice, $\eta=J/(k_B T)$ with J being the coupling constant of the nearest neighbor interaction, and k_B being the Boltzmann constant, and ϵ_i^B are sign factors shown in Table I, and

$$Z_1 = Z_{1/2 \ 1/2}, \quad Z_2 = Z_{1/2 \ 0},$$

$$Z_3 = Z_{0 \ 1/2}, \quad Z_4 = -\text{sgn}(\epsilon)Z_{00}, \quad (3)$$

with

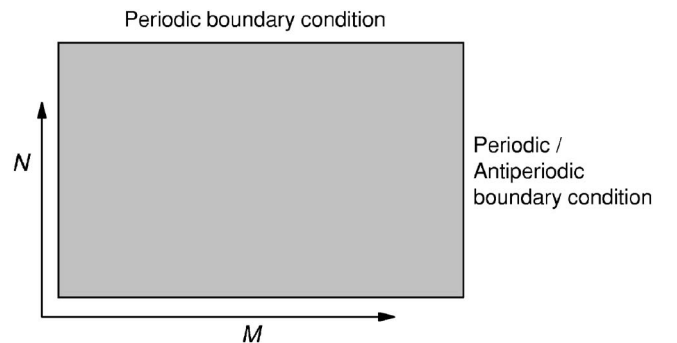


FIG. 1. Illustration for the Ising model on $M \times N$ planar lattice with periodic-periodic and antiperiodic-periodic boundary conditions.

*Electronic address: mcwu@phys.sinica.edu.tw

TABLE I. Sign factors ε_i^B in Eq. (2) for periodic-periodic (pp) and antiperiodic-periodic (ap) boundary conditions.

B.C.	ε_1^B	ε_2^B	ε_3^B	ε_4^B
pp	+	+	+	+
ap	+	-	+	-

$$Z_{\mu\nu} = \prod_{p=0}^{gM-1} \prod_{q=0}^{N-1} \left[\frac{A_0}{A_1} - \cos \frac{2\pi(p+\mu)}{gM} - \cos \frac{2\pi(q+\nu)}{N} - A_2 \cos \left(\frac{2\pi(p+\mu)}{gM} - \frac{2\pi(q+\nu)}{N} \right) \right]^{1/2}. \quad (4)$$

The explicit expressions of A_i for the sq, pt, and hc lattices are shown in Table II.

For the case of an infinite long Ising strip with $N=\infty$, we have $Z_1=Z_2$ and $Z_3=-Z_4$, and the interfacial tension in Eq. (1) becomes

$$\sigma(\epsilon, M) = M[f^a(\epsilon, M) - f^p(\epsilon, M)], \quad (5)$$

where the free energy f^B of a $M \times \infty$ Ising strip can be obtained by taking the limit of $N \rightarrow \infty$ for Eq. (2). The typical behaviors of the interfacial tension σ for the sq, pt, and hc lattices are shown in Figs. 2(a)–2(c), respectively. Here we should note that, as R is approaching to zero gradually, there are strong fluctuations emerged in numerical calculations of Z_i for small R . Due to the existence of the sign factor $\text{sgn}(\epsilon)$ in Eq. (3), the behaviors of the transitions from $M \times N$ to $N \rightarrow \infty$ cannot be observed clearly provided the sign factor is not handled properly. Therefore, no explicit transitive behaviors were reported in Refs. [12,13], due to uncertainties that exist in practical numerical calculations. To overcome this difficulty, we introduce a threshold δ_c , such that as $|Z_1 - Z_2| \leq \delta_c$ or $|Z_3 - Z_4| \leq \delta_c$ then $Z_1=Z_2$ and $Z_3=-Z_4$ should be taken. It follows that for the aspect ratio R ranging from 0.2 to ∞ , the transitive behaviors of the interfacial tensions can be shown explicitly in Fig. 2, in which $\delta_c=10^{-5}$ has been taken for the sq and pt lattices, and 2×10^{-6} for the hc lattice. The jumps appear explicitly in these figures as a consequence of the introduction of δ_c , and their locations depend on the system size, the value of δ_c , and the precision of numerical calculations.

The scaling form of the interfacial tension was proposed to be [12–14]

TABLE II. Expressions for A_0 , A_1 , A_2 , and η_c for various lattices, $t=\tanh(\eta)$.

Lattice	A_0	A_1	A_2	η_c
sq	$(1+t^2)^2$	$2t(1-t^2)$	0	$\frac{1}{2} \ln(1+\sqrt{2})$
pt	$(1+t^2)^3+8t^3$	$2t(1-t^2)^2$	1	$\frac{1}{2} \ln\sqrt{3}$
hc	$1+3t^4$	$2t^2(1-t^2)$	1	$\frac{1}{2} \ln(2+\sqrt{3})$

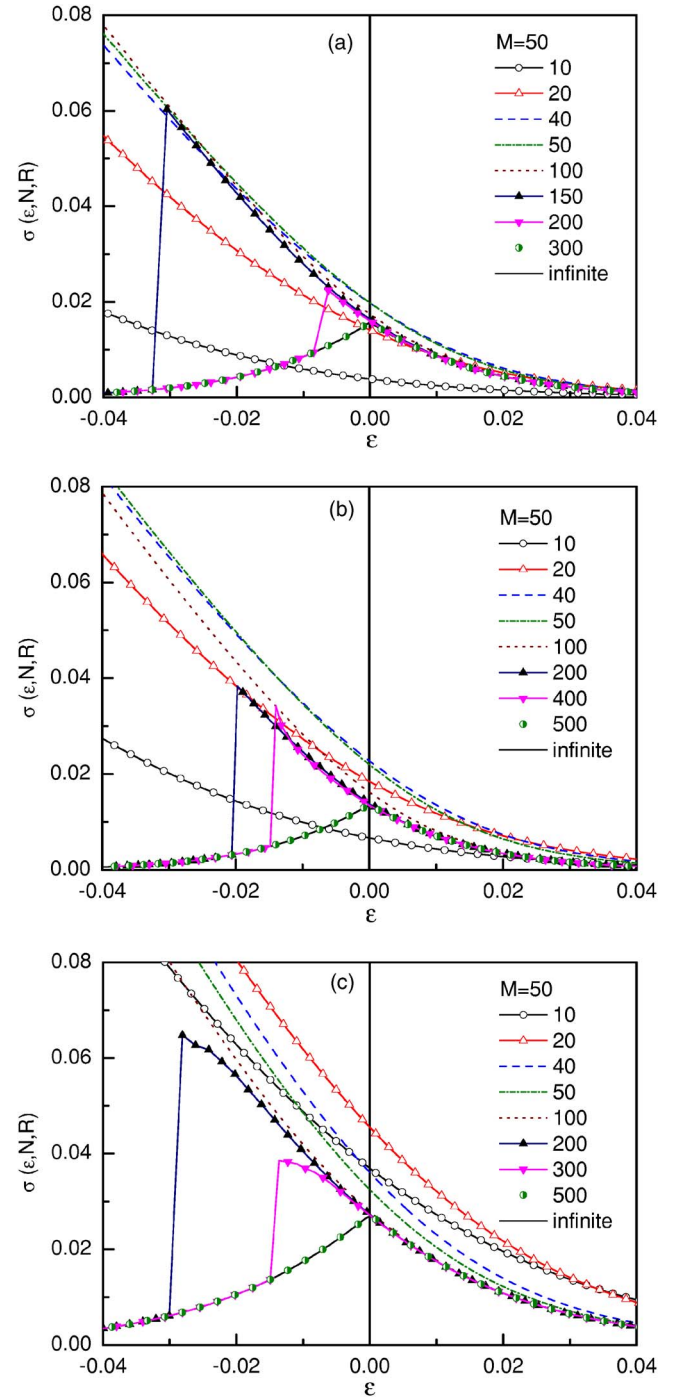


FIG. 2. (Color online) The behaviors of the interfacial tension $\sigma(\epsilon, N, R)$ as a function of ϵ for (a) the sq, (b) pt, and (c) hc lattices with fixed $M=50$, and $N=10, 20, 40, 50, 100, \dots, \infty$.

$$\sigma(\epsilon, R, N) = \frac{1}{N} \Sigma(z, R, N), \quad (6)$$

where $\Sigma(z, R, N)$ with $z=\epsilon N$ is the scaling function. To have an analytical expression of the scaling function, we expand the free energy near the critical point $\epsilon=0$,

TABLE III. Expressions for $c_{0,0}$, $c_{0,1}$, $c_{0,2}$, c_1 , q , $E_{0,0}$, and D ; $\gamma_E(=0.577\ 215\ 664\ 9\dots)$ is the Euler constant.

Lattice	$c_{0,0}$	$c_{0,1}$	$c_{0,2}$	c_1	q	$E_{0,0}$	D
sq	$\frac{8}{\pi}$	$\frac{8}{\pi}(\ln \frac{4\sqrt{2}}{\pi} + \gamma_E - \frac{\pi}{4})$	4	$2\sqrt{2}$	$e^{-\pi R}$	$-\sqrt{2}$	1
pt	$\frac{12\sqrt{3}}{\pi}$	$\frac{12\sqrt{3}}{\pi}(\ln \frac{4\sqrt{3}}{\pi} + \gamma_E - \frac{\sqrt{3}\pi}{6})$	9	6	$e^{-\pi(\sqrt{3}-i)R/2}$	-2	$\frac{\sqrt{3}}{2}$
hc	$\frac{2\sqrt{3}}{\pi}$	$\frac{2\sqrt{3}}{\pi}(\ln \frac{4\sqrt{3}}{\pi} + \gamma_E - \frac{\sqrt{3}\pi}{9})$	$\frac{3}{4}$	$\frac{1}{\sqrt{2}}$	$e^{-\pi(\sqrt{3}-i)R/4}$	$-\frac{2}{\sqrt{3}}$	$\sqrt{3}$

$$f^B(\epsilon, R, N) = f_c^B(0, R, N) - \eta_c E_c^B \epsilon + \frac{1}{2} \left(2\eta_c E_c^B - \frac{C_c^B}{k_B} \right) \epsilon^2 + O(\epsilon^3), \quad (7)$$

where $\eta_c = J/(k_B T_c)$, $E_c^B = (\partial f^B / \partial \eta)_{\epsilon=0}$ is the internal energy, and $C_c^B/k_B = -\eta_c^2 (\partial^2 f^B / \partial \eta^2)_{\epsilon=0}$ is the specific heat at criticality. It follows that the interfacial tension σ can be expanded with respect to z as

$$\Sigma(z, R, N) = \Sigma_0(R, N) + \Sigma_1(R, N)z + \Sigma_2(R, N)z^2 + O(z^3), \quad (8)$$

with

$$\Sigma_0(R, N) = f_c^{ap} - f_c^{pp}, \quad (9)$$

$$\Sigma_1(R, N) = -\eta_c (E_c^{ap} - E_c^{pp}), \quad (10)$$

$$\Sigma_2(R, N) = \eta_c (E_c^{ap} - E_c^{pp}) - \frac{1}{2k_B} (C_c^{ap} - C_c^{pp}). \quad (11)$$

The explicit forms of $\Sigma_0(R, N)$, $\Sigma_1(R, N)$, and $\Sigma_2(R, N)$ can be formulated based on the expansions of f_c^B , E_c^B , and C_c^B with respect to N . The exact expansions of these quantities at a critical point are known as [6]

$$f_c^B = f_{bulk} + \frac{1}{RN^2} [\ln f_1^B - \frac{1}{3} \ln(4f_2)] + O\left(\frac{1}{N^3}\right), \quad (12)$$

$$E_c^B = -E_0 - \frac{1}{N} \sqrt{c_{0,2}} \frac{\epsilon_4^B f_2}{f_1^B} + O\left(\frac{1}{N^2}\right), \quad (13)$$

$$\begin{aligned} \frac{C_c^B}{k_B} &= c_{0,0} \eta_c^2 \ln N + c_{0,1} \eta_c^2 - 2c_{0,0} \eta_c^2 \frac{f_3^B}{f_1^B} - c_{0,2} R \eta_c^2 \left(\frac{f_2}{f_1^B} \right)^2 \\ &\quad - \frac{1}{N} c_1 \eta_c^2 \frac{\epsilon_4^B f_2}{f_1^B} + O\left(\frac{1}{N^2}\right), \end{aligned} \quad (14)$$

where $f_{bulk} = 0.929\ 695\ 4\dots$, for sq, $0.879\ 585\ 4\dots$, for pt, and $1.025\ 059\ 1\dots$, for hc lattices, $f_1^B = \epsilon_1^B |\theta_3| + \epsilon_3^B |\theta_4| + \epsilon_2^B |\theta_2|$, $f_2 = |\theta_2| |\theta_3| |\theta_4|$, $f_3^B = \epsilon_1^B |\theta_3| \ln |\theta_3| + \epsilon_3^B |\theta_4| \ln |\theta_4| + \epsilon_2^B |\theta_2| \ln |\theta_2|$, with $\theta_i = \theta_i(0, q)$ are the Elliptic theta functions of modulus q shown in Table III, and the expressions for E_0 , $c_{0,0}$, $c_{0,1}$, $c_{0,2}$, and c_1 are listed in Table III. Thus, the expressions of $\Sigma_0(R, N)$, $\Sigma_1(R, N)$, and $\Sigma_2(R, N)$, respectively, take the forms

$$\Sigma_0(R, N) = \ln \frac{|\theta_2| + |\theta_3| + |\theta_4|}{-|\theta_2| + |\theta_3| + |\theta_4|} + O\left(\frac{1}{N^2}\right), \quad (15)$$

$$\Sigma_1(R, N) = 2R \sqrt{c_{0,2}} \eta_c \frac{|\theta_2 \theta_3 \theta_4| (|\theta_3| + |\theta_4|)}{(|\theta_3| + |\theta_4|)^2 - |\theta_2|^2} + O\left(\frac{1}{N^2}\right), \quad (16)$$

$$\begin{aligned} \Sigma_2(R, N) &= -4R c_{0,0} \eta_c^2 \frac{|\theta_2| |\theta_3| (\ln |\theta_2| + \ln |\theta_3|)}{(|\theta_3| + |\theta_4|)^2 - |\theta_2|^2} \\ &\quad - 4R c_{0,0} \eta_c^2 \frac{|\theta_2| |\theta_4| (\ln |\theta_2| + \ln |\theta_4|)}{(|\theta_3| + |\theta_4|)^2 - |\theta_2|^2} \\ &\quad - 2R^2 c_{0,2} \eta_c^2 \frac{|\theta_2| |\theta_3 \theta_4|^2 (|\theta_3| + |\theta_4|)}{[(|\theta_3| + |\theta_4|)^2 - |\theta_2|^2]^2} \\ &\quad + \frac{2R}{N} (\sqrt{c_{0,2}} \eta_c + c_1 \eta_c^2) \frac{|\theta_2 \theta_3 \theta_4| (|\theta_3| + |\theta_4|)}{(|\theta_3| + |\theta_4|)^2 - |\theta_2|^2} \\ &\quad + O\left(\frac{1}{N^2}\right). \end{aligned} \quad (17)$$

To explore the behaviors of $\Sigma(0, R, N)$, here we plot the leading terms of $\Sigma_i(R, N)$, denoted by $\Sigma_{i,0}(R)$, as functions of R for the sq, pt, and hc lattices. Figure 3(a) shows the behaviors of $R\Sigma_{0,0}(R)$, in which the result for the sq lattice was first obtained in Ref. [11]. The behaviors of $\Sigma_{1,0}(R)$ as a function of R are shown in Fig. 3(b), and $\Sigma_{2,0}(R)$ are shown in Fig. 3(c). Here we note that Fig. 2 is plotted according to Eq. (1), and Figs. 3(a)–3(c) are plotted based on Eqs. (15)–(17), respectively, and are consistent with results by numerical studies in Refs. [12,13]. The values of $\Sigma_{1,0}(R)$ and $\Sigma_{1,0}(R)$ for a number of aspect ratios can be calculated exactly. For example, in the limit of $N \rightarrow \infty$, or $R \rightarrow 0$, we have, for the sq lattice, the Elliptic theta functions $\theta_2(q, R)$ and $\theta_3(q, R)$ vary as $R^{-1/2}$, and $\theta_4(q, R)$ varies as $2R^{-1/2} e^{-4\pi/(4R)}$, which imply

$$\lim_{R \rightarrow 0} R \Sigma_{0,0}^{sq}(R) = \frac{\pi}{4} = 0.785\ 398\dots \quad (18)$$

Similarly, for the pt and hc lattices, we have

$$\lim_{R \rightarrow 0} R \Sigma_{0,0}^{pt}(R) = \frac{\sqrt{3}}{2} \frac{\pi}{4} = 0.680\ 174\dots, \quad (19)$$

$$\lim_{R \rightarrow 0} R \Sigma_{0,0}^{hc}(R) = \sqrt{3} \frac{\pi}{4} = 1.360\ 349\dots, \quad (20)$$

which can be summarized in a single expression

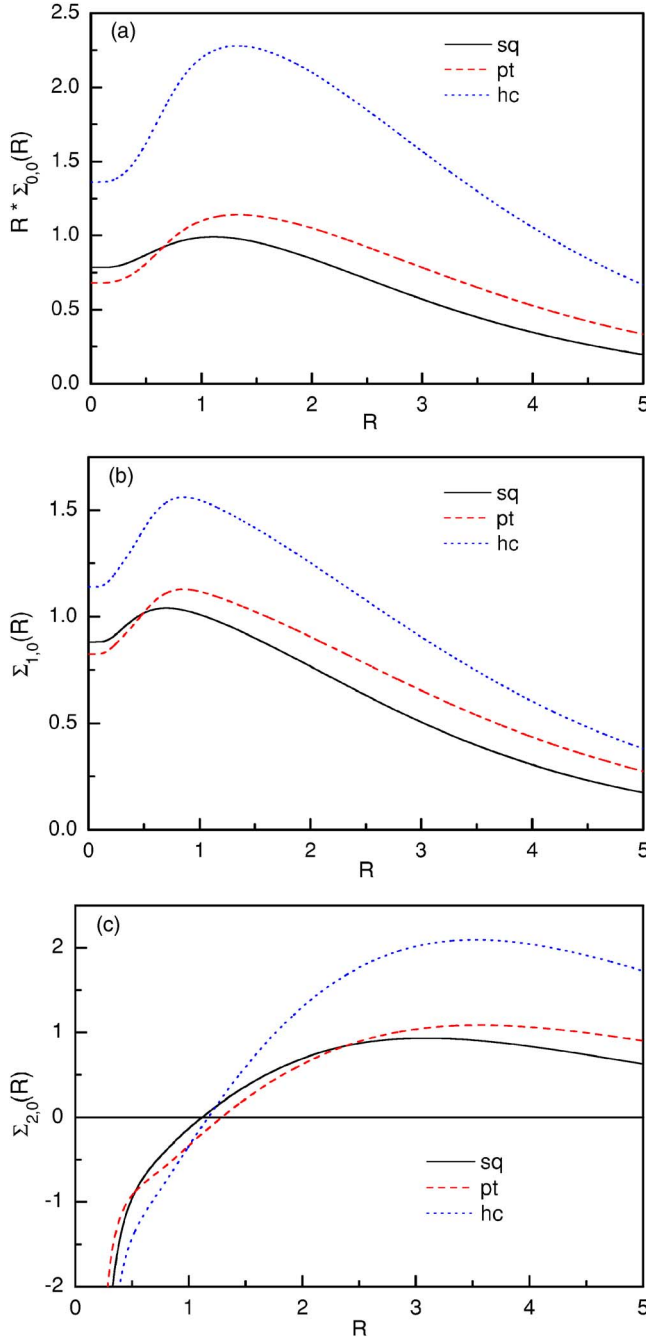


FIG. 3. (Color online) The behaviors of (a) $R \cdot \Sigma_{0,0}(R)$, (b) $\Sigma_{1,0}(R)$, and (c) $\Sigma_{2,0}(R)$ as a function of R for the sq, pt, and hc lattices.

$$\lim_{R \rightarrow 0} R \Sigma_{0,0}(R) = \frac{D\pi}{4}, \quad (21)$$

where the values of D for the sq, pt, and hc lattices are listed in Table III. Following the same procedures, we have

$$\Sigma_{1,0}^{sq}(0) = \ln(1 + \sqrt{2}) = 0.881\,373\dots, \quad (22)$$

$$\Sigma_{1,0}^{pt}(0) = \frac{3}{4} \ln 3 = 0.823\,959\dots, \quad (23)$$

$$\Sigma_{1,0}^{hc}(0) = \frac{\sqrt{3}}{2} \ln(2 + \sqrt{3}) = 1.140\,518\dots, \quad (24)$$

which can also be summarized as a single expression

$$\Sigma_{1,0}(0) = \sqrt{c_{0,2}} \eta_c, \quad (25)$$

where the values of $\sqrt{c_{0,2}}$ and η_c are listed in Table II. For the aspect ratio $R=1$, we have, for the sq lattice, $\theta_2(q^{sq}, 1) = \theta_4(q^{sq}, 1)$, and $\theta_2(q^{sq}, 1)/\theta_3(q^{sq}, 1) = 2^{-1/4}$, and

$$\begin{aligned} \Sigma_{0,0}^{sq}(1) &= \left[\ln \frac{|\theta_2| + |\theta_3| + |\theta_4|}{-|\theta_2| + |\theta_3| + |\theta_4|} \right]_{R=1}^{sq} = \ln(1 + 2^{3/4}) \\ &= 0.986\,486\dots, \end{aligned} \quad (26)$$

which was first obtained in Ref. [11]. Similarly, for the pt and hc lattices, we have $\theta_2(q^{pt,hc}, 1) = \theta_3(q^{pt,hc}, 1) = \theta_4(q^{pt,hc}, 1)$, which leads to

$$\Sigma_{0,0}^{pt}(1) = \ln 3 = 1.098\,612\dots, \quad (27)$$

$$\Sigma_{0,0}^{hc}(1) = 2 \ln 3 = 2.197\,224\dots \quad (28)$$

Furthermore, for $\Sigma_{1,0}(1)$, we have

$$\Sigma_{1,0}^{sq}(1) = 1.009\,92\dots, \quad (29)$$

$$\Sigma_{1,0}^{pt}(1) = 1.117\,74\dots, \quad (30)$$

$$\Sigma_{1,0}^{hc}(1) = 1.547\,17\dots \quad (31)$$

It is interesting that the amplitude of the interfacial tension defined as $R \Sigma_{0,0}$ with $R \rightarrow 0$ for the sq, pt, and hc lattices have relative proportions $1 : \frac{\sqrt{3}}{2} : \sqrt{3}$ which are related to the aspect ratios for the three lattices to have similar domains [8,15]. According to the analytical perspective given above, the relative proportions naturally enter from the modulus q in the corresponding elliptic theta functions, $\theta_i(0, q)$. This demonstrates the origin of the concept of a similar domain. Since Eq. (21) is a conformal result, it is valid for all isotropic Ising lattices.

Here we remark that the treatment of the asymptotic behaviors of a finite lattice system with the aspect ratio $R \rightarrow 0$ has been an important issue to understand the crossover behaviors from a finite-size to a semi-infinite or bulk system. In particular, it is still not quite clear how to handle uncertainties involving the numerical simulations of lattice systems at a criticality at which configuration-averaged quantities usually have a typical accuracy no better than 0.1% due to statistical fluctuations [11]. As a result, some detailed critical behaviors cannot be observed by simulations. Studies of simple models with analytical solutions then become a playground for tackling such problems. In this paper, we have presented a revision of the picture of the interfacial tension at a criticality and the analytical expressions of the amplitudes and the high-order expansions of the scaling function in a unified version. Since our results are rigorous, they provide an important background for extending studies on the fine features of critical lattice systems. For instance, our treatment of the asymptotic behaviors and the analytical expressions are helpful for the investigations of the existence of

discontinuities of thermodynamic quantities at a criticality of infinitely long Ising cylinders with an antiperiodically joined circumference [16]. Furthermore, although the results of our study are based on analytical solutions, the formulations presented in this paper can be extended to numerical or experimental studies of finite critical systems [17].

The present work also inspires similar and further study in the dimer model, where the interfacial tension can be extensively defined as the difference between the free energies of the dimer models, respectively, with lattice sizes of $2M \times 2N$ and $2M \times (2N+1)$. Quite recently, Izmailian *et al.* [18] showed that the finite-size corrections in two-dimensional dimer models on square lattices should be interpreted by the effective central charge instead of a central charge such that the effects from changes of parity and boundary conditions

in the dimer model can be interpreted consistently. Nevertheless, the transitions among different lattice spaces are still unclear and require further studies. Since the central charge parametrizing two-dimensional critical systems is directly related to finite-size corrections to the critical free energy, the analysis of interfacial tension shall be a way to understand the transitive behaviors of the triangular dimer model at the critical point at which it becomes the square lattice [19]. The formulations and analytical expressions presented in this paper are a useful reference for such studies.

This work was partially supported by Academia Sinica, Taiwan. The author thanks Professor M.-C. Huang, Professor C.-K. Hu, Professor F.-Y. Wu, and Dr. N. Sh. Izmailian for helpful discussions.

-
- [1] For a review, see *Finite-size Scaling and Numerical Simulation of Statistical Systems*, edited by V. Privman (World Scientific, Singapore, 1990).
- [2] A. E. Ferdinand and M. E. Fisher, *Phys. Rev.* **185**, 832 (1969).
- [3] C.-K. Hu, *Phys. Rev. B* **29**, 5103 (1984); C.-K. Hu, C.-Y. Lin, and J.-A. Chen, *Phys. Rev. Lett.* **75**, 193 (1995); **75**, 2786(E) (1995); *Physica A* **221**, 80 (1995); C.-K. Hu and C.-Y. Lin, *Phys. Rev. Lett.* **77**, 8 (1996); H.-P. Hsu, S. C. Lin, and C.-K. Hu, *Phys. Rev. E* **64**, 016127 (2001); H. Watanabe, S. Yukawa, N. Ito, and C.-K. Hu, *Phys. Rev. Lett.* **93**, 190601 (2004); H. Watanabe and C.-K. Hu, *ibid.* **95**, 258902 (2005).
- [4] Y. Okabe, K. Kaneda, M. Kikuchi, and C.-K. Hu, *Phys. Rev. E* **59**, 1585 (1999); Y. Tomita, Y. Okabe, and C.-K. Hu, *ibid.* **60**, 2716 (1999); C.-K. Hu, J.-A. Chen, and C.-Y. Lin, *Physica A* **266**, 27 (1999).
- [5] C.-K. Hu, J.-A. Chen, N. Sh. Izmailian, and P. Kleban, *Phys. Rev. E* **60**, 6491 (1999); N. Sh. Izmailian and C.-K. Hu, *Phys. Rev. Lett.* **86**, 5160 (2001); W.-T. Lu and F. Y. Wu, *Phys. Rev. E* **63**, 026107 (2001); K. Kaneda and Y. Okabe, *Phys. Rev. Lett.* **86**, 2134 (2001); N. Sh. Izmailian and C.-K. Hu, *Phys. Rev. E* **65**, 036103 (2002); W. Janke and R. Kenna, *Phys. Rev. B* **65**, 064110 (2002); N. Sh. Izmailian, K. B. Oganesyan, and C.-K. Hu, *Phys. Rev. E* **65**, 056132 (2002).
- [6] E. V. Ivashkevich, N. Sh. Izmailian, and C.-K. Hu, *J. Phys. A* **35**, 5543 (2002); J. Salas, *ibid.* **34**, 1311 (2001); **35**, 1833 (2002).
- [7] V. Privman and M. E. Fisher, *Phys. Rev. B* **30**, 322 (1984); K.-C. Lee, *Phys. Rev. Lett.* **69**, 9 (1992).
- [8] M.-C. Wu, C.-K. Hu, and N. Sh. Izmailian, *Phys. Rev. E* **67**, 065103(R) (2003).
- [9] M.-C. Wu and C.-K. Hu, *J. Phys. A* **35**, 5189 (2002).
- [10] V. Privman and J. Rudnick, *J. Phys. A* **19**, L1215 (1986).
- [11] H. Park and M. den Nijs, *Phys. Rev. B* **38**, 565 (1988).
- [12] M.-C. Wu, M.-C. Huang, Y.-P. Luo, and T.-M. Liaw, *J. Phys. A* **32**, 4897 (1999).
- [13] T.-M. Liaw, M.-C. Huang, S. C. Lin, and M.-C. Wu, *Phys. Rev. B* **60**, 12994 (1999).
- [14] K. K. Mon and D. Jasnow, *Phys. Rev. A* **30**, 670 (1984).
- [15] R. P. Langlands, C. Pichet, P. Pouliot, and Y. Saintaubin, *J. Stat. Phys.* **67**, 553 (1992).
- [16] This issue arises from the treatments of thermodynamical quantities at criticality, and is still an unsolved problem. See, e.g., T.-M. Liaw, M.-C. Huang, S. C. Lin, and Y.-P. Luo, e-print cond-mat/0408393.
- [17] H. Hilgenkamp, Ariando, H. J. H. Smilde, D. H. A. Blank, G. Rijnders, H. Rogalla, J. R. Kirtley, and C.-C. Tsuei, *Nature (London)* **422**, 50 (2003).
- [18] N. Sh. Izmailian, V. B. Priezzhev, P. Ruelle, and C.-K. Hu, *Phys. Rev. Lett.* **95**, 260602 (2005).
- [19] N. Sh. Izmailian, K. B. Oganesyan, M.-C. Wu, and C.-K. Hu, *Phys. Rev. E* **73**, 016128 (2006).